Supplementary Figures

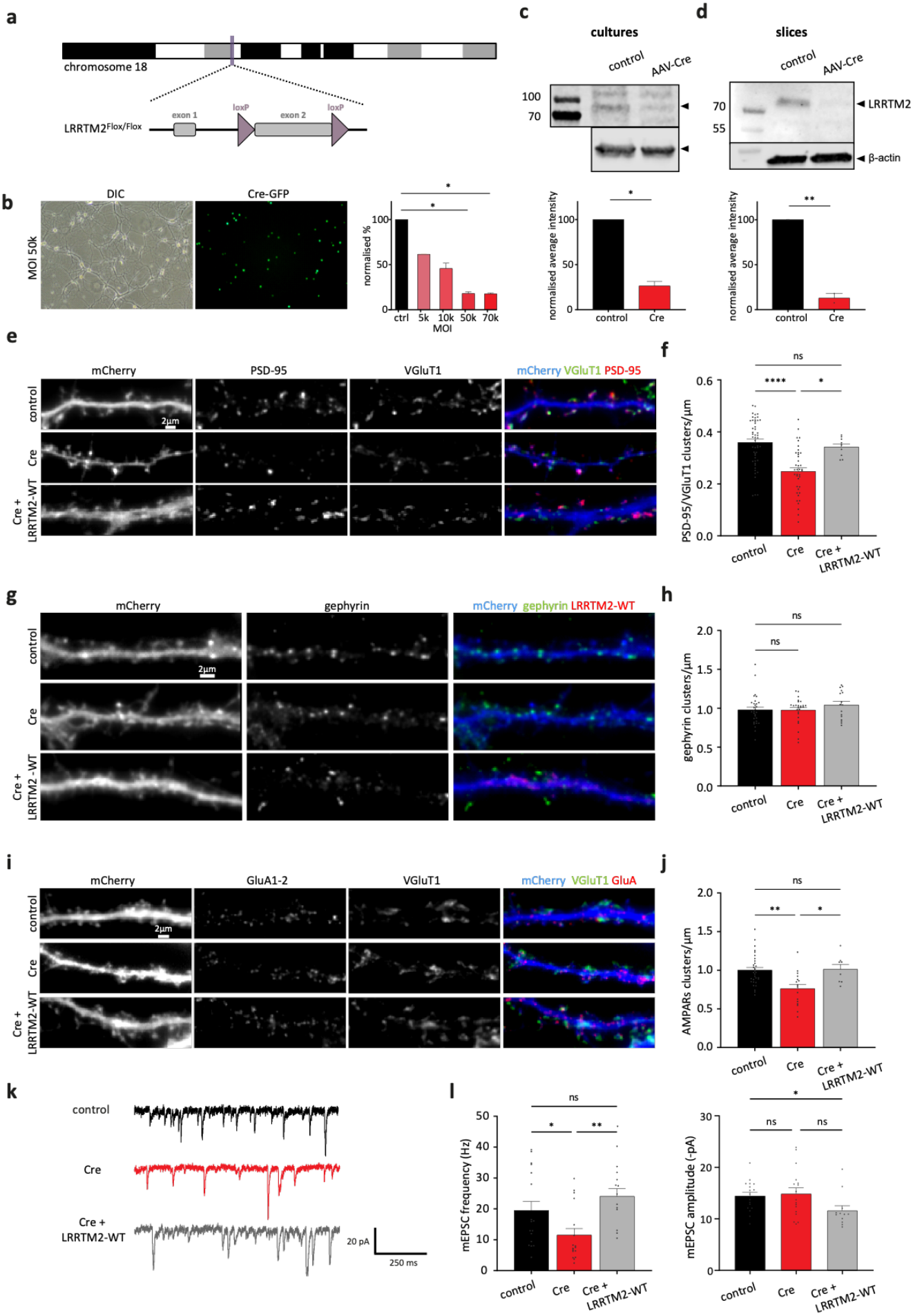

Supplementary Figure 1. Conditional knock-out of LRRTM2 impairs excitatory synapse development and function.

(a) Schematics of LRRTM2 gene locus in mouse chromosome 18. Purple inset shows the 2 exons of LRRTM2 gene and the insertion of loxP sites upstream and downstream of exon 2. (b) Representative images of cultured hippocampal neurons from LRRTM2$^{Flox/Flox}$ mice infected with nuclear Cre-GFP-encoding virus and RT-qPCR quantification of LRRTM2 RNA expression in control (control) or in neurons infected with increasing dose of Cre-GFP virus (MOI: 5k, 10k, 20k, 50k and 70k). Data acquired from 2 experiments for each condition. MOI: multiplicity of infection, * $p<0.05$. (c) LRRTM2 and β-actin immunoblots of proteins extracted from hippocampal LRRTM2$^{Flox/Flox}$ cultures. Data presented as mean +/- sem, obtained from 3 independent experiments, * $p<0.05$, compared by unpaired t-test. (d) LRRTM2 and β-actin immunoblots of proteins extracted from organotypic hippocampal slices not infected (control) or infected with an AAV-Cre virus (AAV-Cre). Data presented as mean +/- sem, obtained from 2 experiments ** $p<0.01$ compared by unpaired t-test. (e) DIV15 hippocampal neurons expressing mCherry (control), Cre-mCherry (Cre) or Cre-mCherry and biotinylated AP-LRRTM2 (Cre+LRRTM2-WT) immunostained for endogenous PSD-95 and VGlut1 as post- and pre-synaptic markers, respectively. Right, Cre-mCherry (blue) overlaid with PSD-95 (red) and VGluT1 (green). (f) Quantification of synaptic density measured as the apposition of PSD-95 and VGluT1 puncta. Data acquired from 3 (control: n=49, Cre: n=38 cells) and 2 independent experiments (Cre + LRRTM2-WT: n=9 cells) * $p<0.05$, **** $p<0.0001$. (g) DIV15 hippocampal neurons expressing mCherry (control), Cre-mCherry (Cre) or Cre-mCherry and biotinylated AP-LRRTM2 (Cre + LRRTM2-WT) immunostained for endogenous gephyrin as marker of inhibitory synapses. Right, Cre-mCherry (blue) overlaid with gephyrin (green) and for the Cre + LRRTM2-WT condition, with AP-LRRTM2 (red). (h) Quantification of inhibitory synaptic density measured as the number of gephyrin clusters/µm. Data acquired from 2 independent experiments (control: n=30, Cre: n=26, Cre + LRRTM2-WT=16 cells). (i) DIV15 hippocampal neurons expressing mCherry (control), Cre-mCherry (Cre) or Cre-mCherry and biotinylated AP-LRRTM2 (Cre + LRRTM2-WT) immunostained for endogenous GluA1/2 subunits of AMPARs and VGluT1. Right, Cre-Cherry (blue) overlaid with GluA1/2 (red) and VGluT1 (green). (j) Quantification of normalized AMPARs density showing significant decrease of AMPAR cluster density in the absence of LRRTM2. Data acquired from 3 independent experiments (control: n=31, Cre: n=16, Cre + LRRTM2-WT=8 cells), * $p<0.05$, ** $p<0.01$. (k) Representative mEPSC traces recorded from DIV15 hippocampal neurons expressing mCherry (control), Cre-mCherry (Cre) or Cre-mCherry and biotinylated AP-LRRTM2 (Cre + LRRTM2-WT). (l) mean mEPSC frequency for control, Cre, and Cre + LRRTM2-WT showing a decreased frequency, but no change in mEPSC amplitude in the cKO compared to control condition. Data acquired from 3 (control: n=17, Cre: n=17 cells) and 2 independent experiments (Cre + LRRTM2-WT n=13 cells), * $p<0.05$, **$p<0.01$. Data are presented as mean values +/- SEM. (b,f,j,l) Data were compared by one-way analysis of variance test, followed by post-hoc Dunn's test.

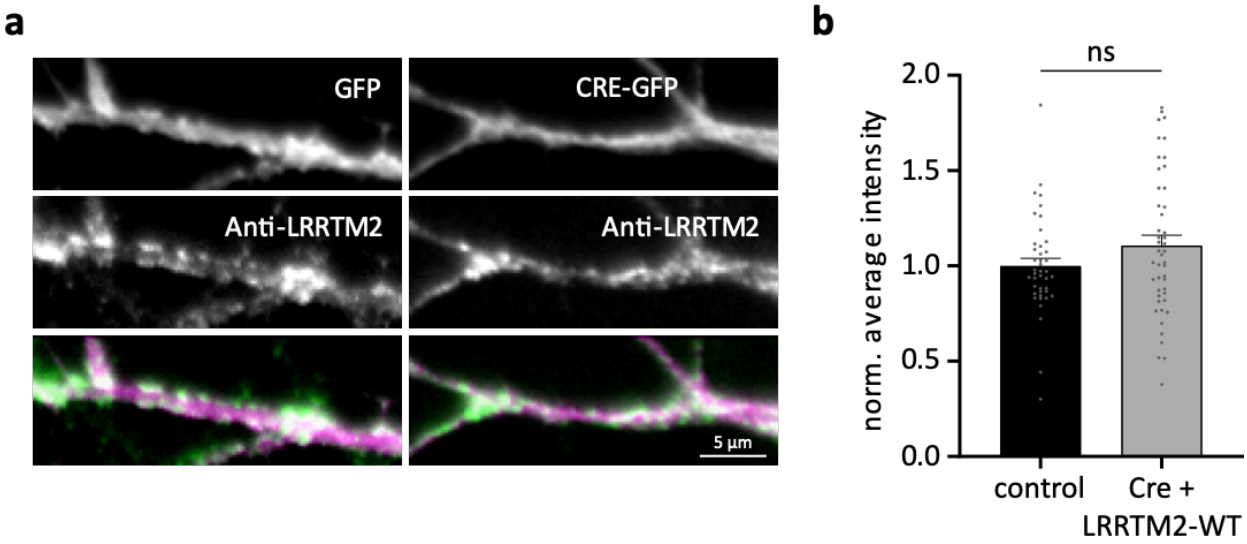

Supplementary Figure 2. LRRTM2 expression on cKO background is similar to endogenous levels.

(a) DIV15 hippocampal neurons expressing GFP (control) or Cre-GFP and biotinylated AP-LRRTM2 (Cre + LRRTM2-WT) immunostained for LRRTM2 after glyoxal fixation and (b) normalized average intensity of LRRTM2 expression in each conditions, showing no significant change in protein expression. Data acquired from 3 independent experiments (control, n=42 cells, Cre + LRRTM2-WT n=47 cells). Data are presented as mean values +/- SEM. Data were compared by non-parametric Mann-Whitney test.

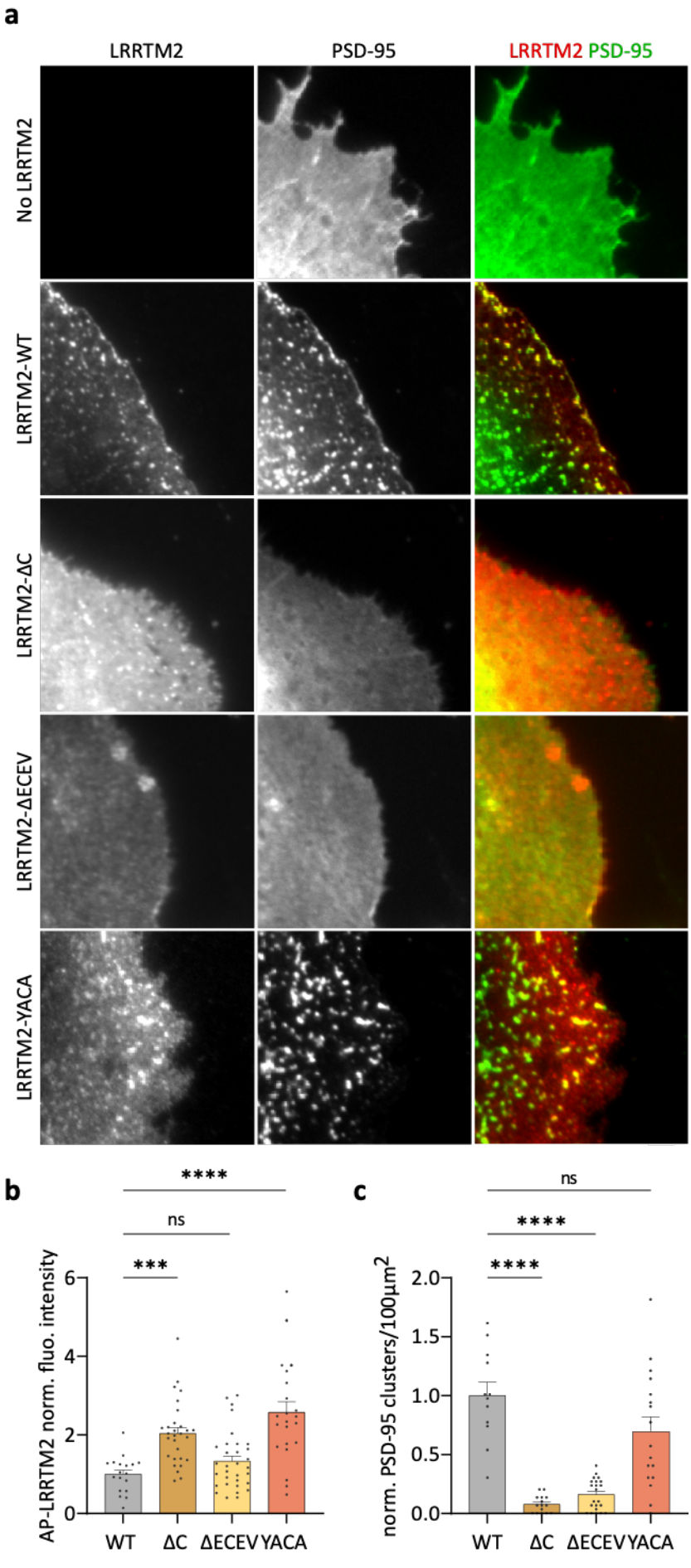
a
LRRTM2
PSD-95
LRRTM2 PSD-95
No LRRTM2
LRRTM2-WT
LRRTM2-ΔC
LRRTM2-ΔECEV
LRRTM2-YACA
b
****
ns
***
AP-LRRTM2 norm. fluo. intensity
0
2
4
6
WT
ΔC
ΔECEV
YACA
c
ns
****
****
norm. PSD-95 clusters/100µm2
0.0
0.5
1.0
1.5
2.0
WT
ΔC
ΔECEV
YACA

Supplementary Figure 3. LRRTM2 and PSD-95 co-cluster through the ECEV motif.

(a) COS-7 cells expressing intracellular mutants of AP-LRRTM2, BirA^{ER}, and PSD-95-GFP (middle) surface labeled with ATTO565-conjugated monomeric streptavidin, ATTO565-mSA (left). Notice the homogeneous distribution of PSD-95 in the absence of LRRTM2 (top). On the right, AP-LRRTM2 mutants (red) are overlaid with PSD-95-GFP (green). (b) Normalized fluoresce intensity of AP-LRRTM2 mutants showing an increase in surface expression for the ΔC and the YACA. (c) Quantification of the PSD-95 density per cell for the different conditions showing that LRRTM2 and PSD-95 co-cluster through the intracellular ECEV motif. Data obtained from 2 experiments (WT: n=12; ΔC n=19; ΔECEV: n=23; YACA: n=17 cells), *** $p<0.001$, **** $p<0.0001$. Data are presented as mean values +/- SEM. Data were compared by one-way analysis of variance test, followed by post hoc Dunn's test.

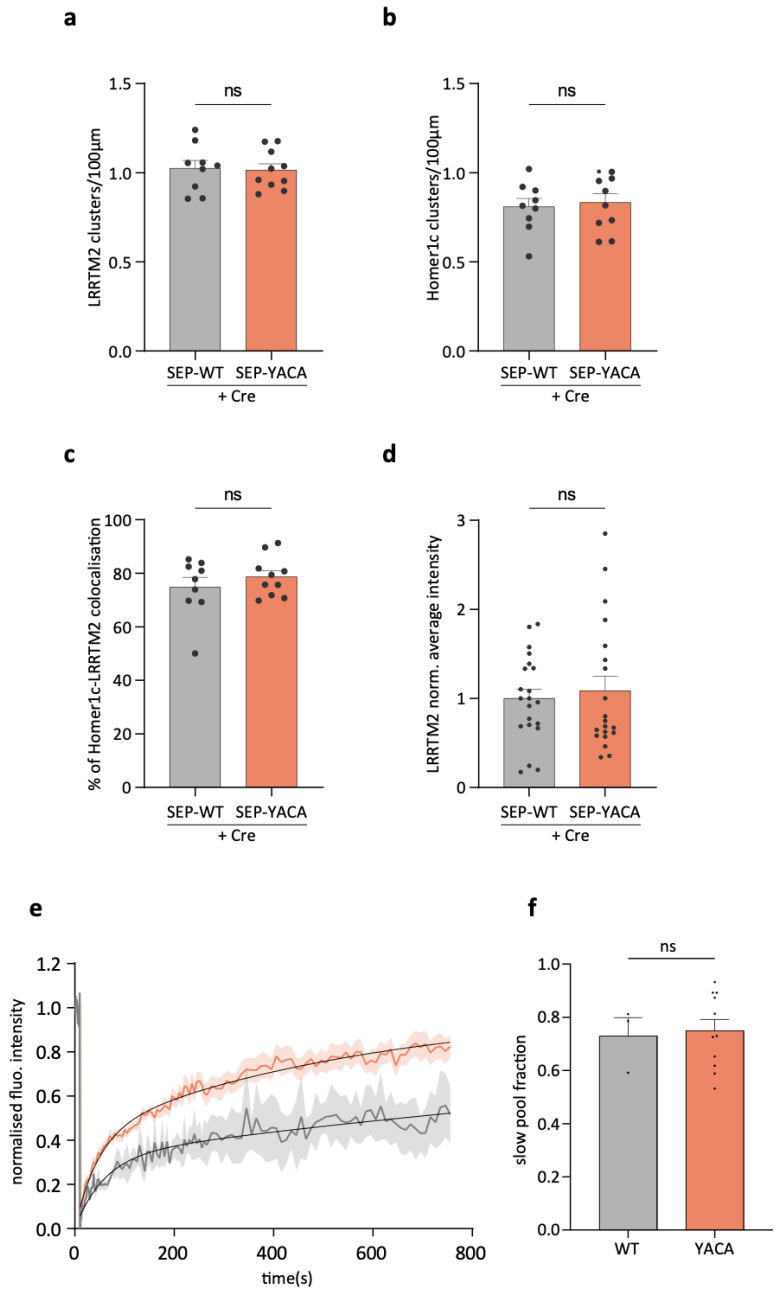

Supplementary Figure 4. SEP-LRRTM2-YACA and SEP-LRRTM2-WT are equally localized to synapses.

(a) Quantification of SEP-LRRTM2-WT and SEP-LRRTM2-YACA cluster density. (b) Quantification of Homer1c-BFP cluster density for SEP-LRRTM2-WT and SEP-LRRTM2-YACA. (c) Percentage of Homer1c-BFP and SEP-LRRTM2-WT or SEP-LRRTM2-YACA colocalization. Data obtained from 3 independent experiments (SEP-LRRTM2-WT n=9; SEP-LRRTM2-YACA n=10 cells). (d) Normalized average intensity of SEP-WT and SEP-YACA. Data obtained from 3 independent experiments (SEP-LRRTM2-WT n=21; SEP-LRRTM2-YACA n=20 cells). (e) FRAP recovery curves outside synapses and (f) corresponding slow pool fractions extracted from FRAP curve fitting. Data acquired from 3 independent experiments (SEP-LRRTM2-WT n=3 regions, SEP-LRRTM2-YACA n=11 regions). Data are presented as mean values +/- SEM. Data were compared by non-parametric Mann-Whitney test.

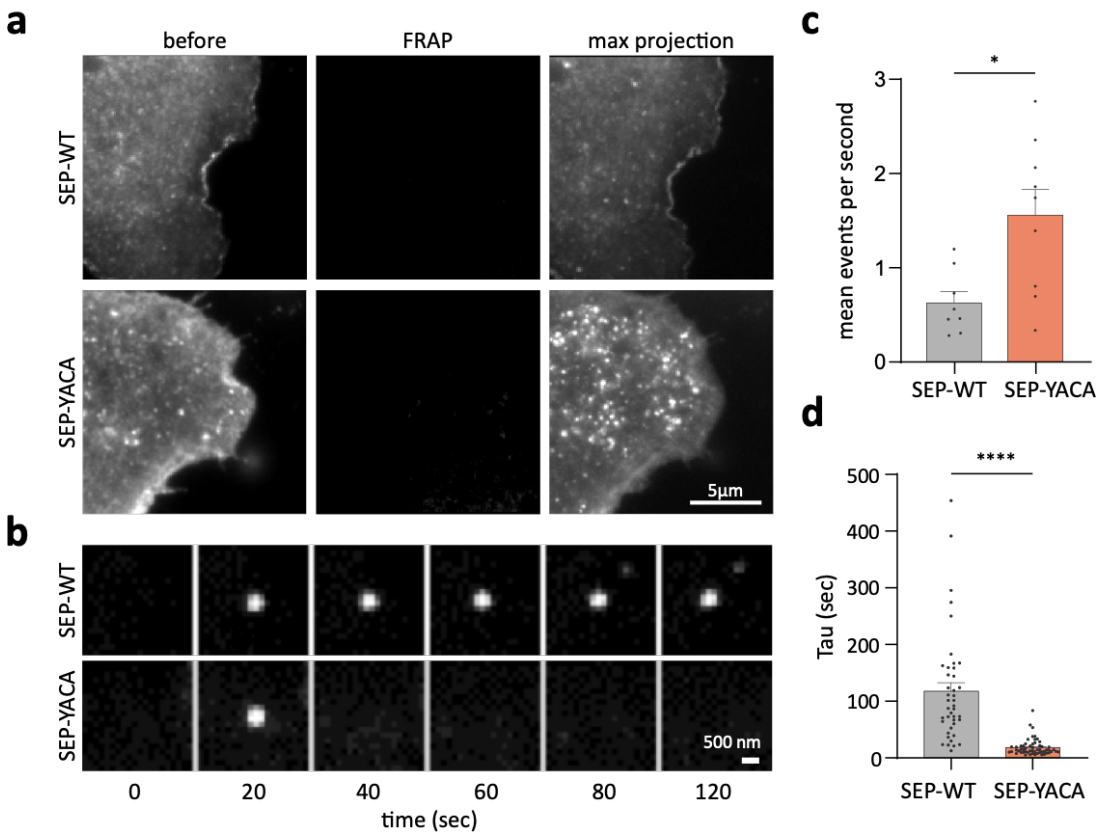

Supplementary Figure 5. The C-terminal YxxC motif regulates LRRTM2 exocytosis in COS-7 cells.

(a) Representative images of COS-7 cells expressing SEP-LRRTM2-WT or SEP-LRRTM2-YACA (left). After photobleaching of all surface proteins (middle), individual exocytic events were monitored with time-lapse imaging. Maximum projection of the frames acquired is depicted in the right panel, showing drastic increase in exocytic events in the SEP-LRRTM2-YACA condition. (b) Examples of individual exocytic events of SEP-LRRTM2-WT and SEP-LRRTM2-YACA. (c) Quantification of the mean number of exocytic events per second per field of view. (d) Rate of fluorescence decay of individual exocytic events. Data acquired from 2 experiments. SEP-LRRTM2-WT: n=8 cells, SEP-LRRTM2-YACA: n=9 cells, * $p<0.05$, **** $p<0.0001$. Data are presented as mean values +/- SEM. Data were compared by non-parametric Mann-Whitney test.

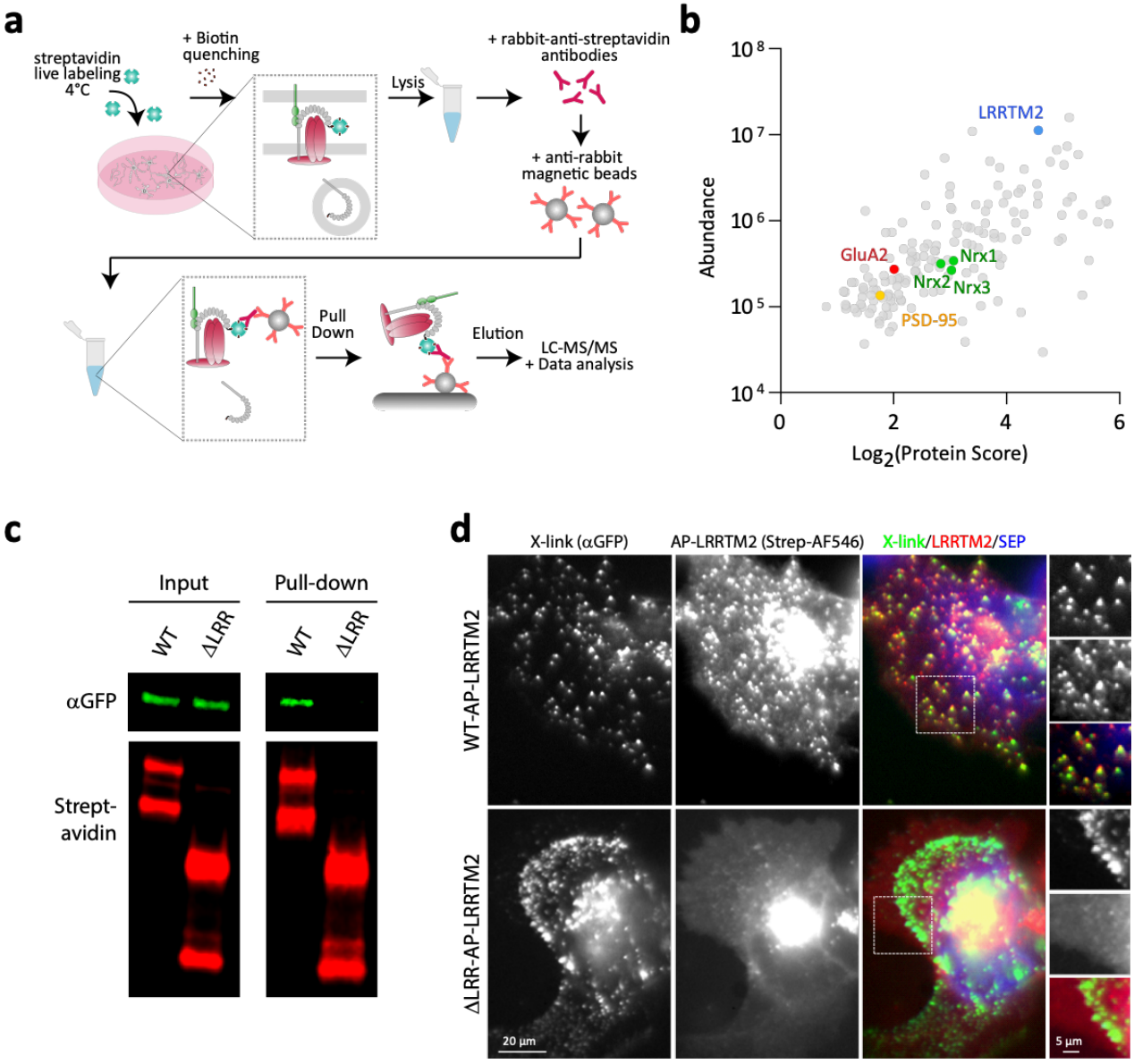

Supplementary Figure 6. AMPARs are present in LRRTM2 surface proteome.

(a) Schematics showing the strategy for selective targeting of LRRTM2 surface interactome. Cells were incubated with streptavidin 40 min at 4°C to prevent internalization, and quenched with biotin (5 min) before lysis. Anti-streptavidin antibodies were used to target surface-streptavidin-labeled LRRTM2 followed by incubation with anti-rabbit-coated magnetic bead incubation OVN at 4°C. A magnetic holder was used to immobilized pulled-down beads for washes, before sample elution and LC-MS/MS analysis (b) Mass spectrometry interaction screen showing the presence of AMPAR subunit GluA2 in the surface proteome of LRRTM2. The data are plotted as a measure of protein abundance versus protein score calculated as the sum of the negative log of the posterior error probability of connected peptide-spectrum matches. Each dot in the scatter plot represents a protein identified by mass spectrometry. The blue dot is LRRTM2 (bait protein), the green dots are Neurexin family members 1-3, known to interact with LRRTM2, the yellow dot represents PSD-95, also known interactor of LRRTM2, and the red dot represents GluA2. Gray dots represent other proteins that were also identified (see Table S1). (c) Representative Western blot showing input and co-precipitation of SEP-GluA2 by streptavidin pull-down in COS-7 cells expressing SEP-GluA2, BirA^{ER}, and WT-AP-LRRTM2 or ΔLRR-AP-LRRTM2. SEP-GluA2 co-precipitates in the presence of WT-LRRTM2 but not ΔLRR-LRRTM2 (n=2 independent experiments). (d) Representative images of live co-recruitment assays in COS-7 cells expressing SEP-GluA2, BirA^{ER}, and WT-AP-LRRTM2 or ΔLRR-AP-LRRTM2 (n=2 independent experiments, 30 cells per condition). SEP-GluA2 was cross-linked with secondary and primary antibodies against GFP, and LRRTM2 co-recruitment to these clusters was assessed by live imaging. WT-LRRTM2, but not ΔLRR-LRRTM2 co-segregated with GluA2.

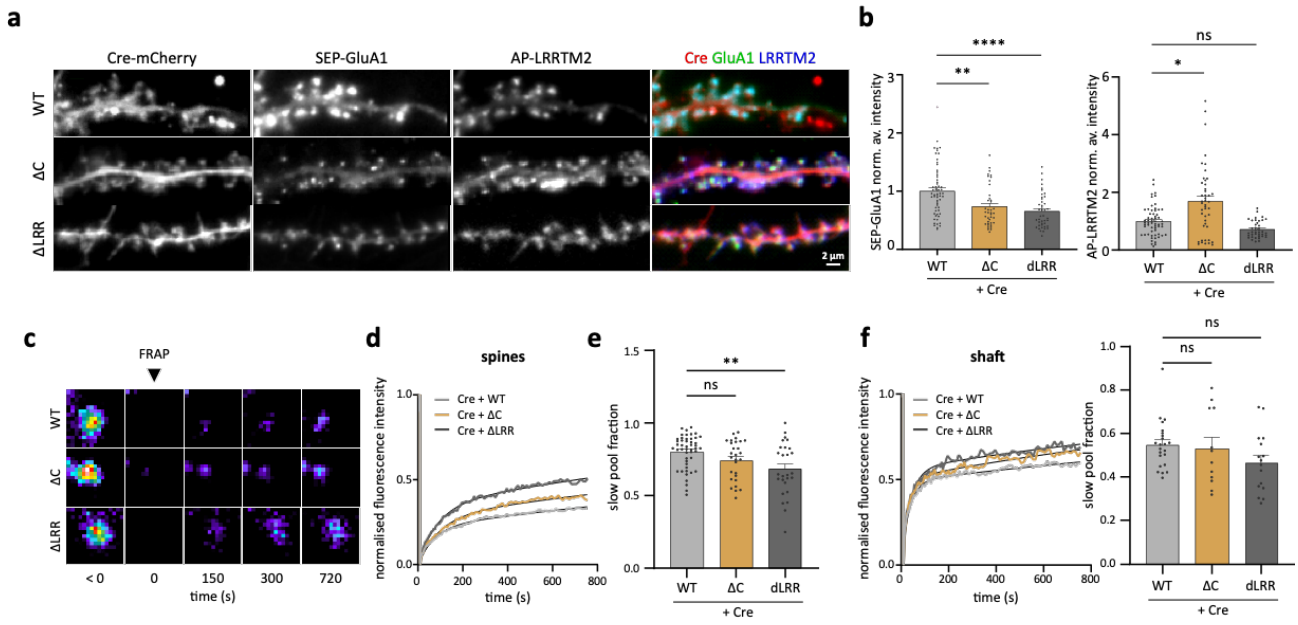

Supplementary Figure 7. AP-LRRTM2 controls AMPARs stabilization via its extracellular region.

(a) DIV15 hippocampal neurons expressing Cre-mCherry, BirA^{ER}, SEP-GluA1 and LRRTM2-WT (WT), LRRTM2-ΔC (ΔC) or LRRTM2-ΔLRR (ΔLRR). On the right, mCherry (red) is overlaid with SEP-GluA1 (green) and the different LRRTM2 constructs (blue). (b) Normalized expression levels of SEP-GluA1 in FRAP regions, and normalized surface intensity of AP-LRRTM2 in each condition. (c) FRAP experiments on spine-accumulated SEP-GluA1 expressing Cre-mCherry and AP-LRRTM2 mutants showing a faster recovery in the ΔLRR condition. (d) Normalized fluorescence recovery curves in spines showing an intermediate recovery for the ΔC, and (e) corresponding slow pool fraction extracted from FRAP curve fitting, showing a reduction of the slow pool fraction only in the ΔLRR condition. (f) Normalized fluorescence recovery curves in shaft regions showing no difference in the recovery rates or in the slow pool fractions. Data obtained from 3 independent experiments. (spines WT: 51; ΔC: 28; ΔLRR: 27 regions; shaft WT: 23; ΔC: 12; ΔLRR: 16 regions), * p<0.05, ** p<0.01, **** p<0.0001. Data are presented as mean values +/- SEM. Data were compared by one-way analysis of variance test, followed by post hoc Dunn's test.

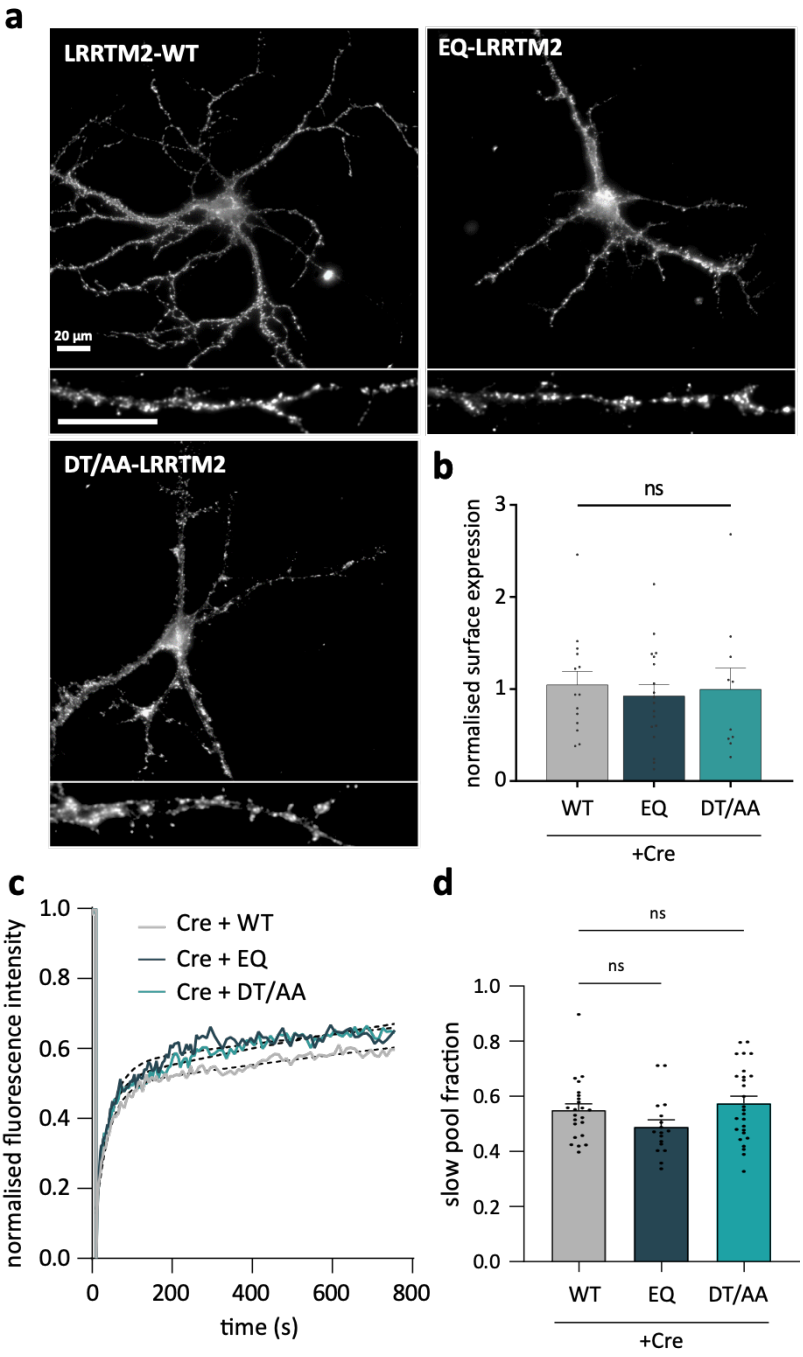

Supplementary Figure 8. LRRTM2 extracellular mutants display similar expression levels.

(a) Representative images of DIV15 hippocampal neurons expressing Cre-mCherry, BirA^{ER} and biotinylated AP-LRRTM2 (WT, EQ or DT/AA). Insets depict labeling of LRRTM2 mutants at the surface of individual dendrites. (b) Normalized fluorescence intensity showing no change in expression of the mutants at the plasma membrane of neurons. Data obtained from 2 independent experiments (WT: 14, EQ: n= 18, DT/AA: n= 10 cells). (c) Normalized fluorescence intensity of fluorescence recovery for SEP-GluA1 in regions outside synapses and (d) corresponding slow pool fractions of SEP-GluA1 extracted from FRAP curve fitting showing no differences between conditions. Data are presented as mean values +/- SEM. Data were compared by one-way analysis of variance test, followed by post hoc Dunn's test.

Gene Symbol	Description	Accession
Tuba1a	Tubulin alpha-1A	P68369
Myh9	Myosin-9	Q8VDD5
Tuba4a	Tubulin alpha-4A	P68368
Myh10	Myosin-10	Q61879
Tubb5	Tubulin beta-5	P99024
Tubb2a	Tubulin beta-2A	Q7TMM9
Tubb2b	Tubulin beta-2B	Q9CWF2
Tubb4b	Tubulin beta-4B	P68372
Tubb3	Tubulin beta-3	Q9ERD7
Camk2a	Calcium/calmodulin-dependent protein kinase type II subunit alpha	P11798
Atp1a3	Sodium/potassium-transporting ATPase subunit alpha-3	Q6PIC6
Atp1a1	Sodium/potassium-transporting ATPase subunit alpha-1	Q8VDN2
Atp5f1a	ATP synthase subunit alpha, mitochondrial	Q03265
Lrrtm2	Leucine-rich repeat transmembrane neuronal protein 2	Q8BGA3
Eno1	Alpha-enolase	P17182
Actg1	Actin, cytoplasmic 2	P63260
Actb	Actin, cytoplasmic 1	P60710
Ywhaz	14-3-3 protein zeta/delta	P63101
Slc25a4	ADP/ATP translocase 1	P48962
Atp1a2	Sodium/potassium-transporting ATPase subunit alpha-2	Q6PIE5
Ywhaq	14-3-3 protein theta	P68254
Atp5f1b	ATP synthase subunit beta, mitochondrial	P56480
Ywhag	14-3-3 protein gamma	P61982
Gfap	Glial fibrillary acidic protein	P03995
Hsp90ab1	Heat shock protein HSP 90-beta	P11499
Prdx6	Peroxiredoxin-6	O08709
Nsf	Vesicle-fusing ATPase	P46460
Ywhah	14-3-3 protein eta	P68510
Slc25a5	ADP/ATP translocase 2	P51881
Gstm1	Glutathione S-transferase Mu 1	P10649
Basp1	Brain acid soluble protein 1	Q91XV3
Pkm	Pyruvate kinase PKM	P52480
Trim21	E3 ubiquitin-protein ligase TRIM21	Q62191
Hspa8	Heat shock cognate 71 kDa protein	P63017
Sptan1	Spectrin alpha chain, non-erythrocytic 1	P16546
Atp6v1b2	V-type proton ATPase subunit B, brain isoform	P62814
Myh14	Myosin-14	Q6URW6
Hsp90aa1	Heat shock protein HSP 90-alpha	P07901
Ywhab	14-3-3 protein beta/alpha	Q9CQV8
Glud1	Glutamate dehydrogenase 1, mitochondrial	P26443
Ckb	Creatine kinase B-type	Q04447
Ppp3ca	Serine/threonine-protein phosphatase 2B catalytic subunit alpha isoform	P63328
Tpi1	Triosephosphate isomerase	P17751
Gpi	Glucose-6-phosphate isomerase	P06745
Pdhx	Pyruvate dehydrogenase protein X component, mitochondrial	Q8BKZ9
Itm2c	Integral membrane protein 2C	Q91VK4
Sptbn1	Spectrin beta chain, non-erythrocytic 1	Q62261
Coro1c	Coronin-1C	Q9WUM4
Hspa2	Heat shock-related 70 kDa protein 2	P17156

Gene Symbol	Description	Accession
Pdia3	Protein disulfide-isomerase A3	P27773
Fscn1	Fascin	Q61553
Nrxn2	Neurexin-2	E9Q7X7
C1qb	Complement C1q subcomponent subunit B	P14106
Uba52	Ubiquitin-60S ribosomal protein L40	P62984
Camk2b	Calcium/calmodulin-dependent protein kinase type II subunit beta	P28652
C1qa	Complement C1q subcomponent subunit A	P98086
C1qc	Complement C1q subcomponent subunit C	Q02105
Atp1b1	Sodium/potassium-transporting ATPase subunit beta-1	P14094
Dbn1	Drebrin	Q9QXS6
Eef1g	Elongation factor 1-gamma	Q9D8N0
Rab3a	Ras-related protein Rab-3A	P63011
Dpysl3	Dihydropyrimidinase-related protein 3	Q62188
Gapdh	Glyceraldehyde-3-phosphate dehydrogenase	P16858
Aldoa	Fructose-bisphosphate aldolase A	P05064
Nrxn1	Neurexin-1	Q9CS84
Nrxn3	Neurexin-3	Q6P9K9
Actr3	Actin-related protein 3	Q99JY9
Phb	Prohibitin	P67778
Aldh2	Aldehyde dehydrogenase, mitochondrial	P47738
Aco2	Aconitate hydratase, mitochondrial	Q99KI0
Eef1a1	Elongation factor 1-alpha 1	P10126
Dnajb6	DnaJ homolog subfamily B member 6	O54946
Hspa1a	Heat shock 70 kDa protein 1A	Q61696
Eno2	Gamma-enolase	P17183
Ywhae	14-3-3 protein epsilon	P62259
Slc25a3	Phosphate carrier protein, mitochondrial	Q8VEM8
Rab3c	Ras-related protein Rab-3C	P62823
Gstm5	Glutathione S-transferase Mu 5	P48774
Uchl1	Ubiquitin carboxyl-terminal hydrolase isozyme L1	Q9R0P9
Prdx1	Peroxiredoxin-1	P35700
Ppm1h	Protein phosphatase 1H	Q3UYC0
Pygb	Glycogen phosphorylase, brain form	Q8CI94
Mdh2	Malate dehydrogenase, mitochondrial	P08249
Idh3a	Isocitrate dehydrogenase [NAD] subunit alpha, mitochondrial	Q9D6R2
Dsp	Desmoplakin	E9Q557
Vdac3	Voltage-dependent anion-selective channel protein 3	Q60931
Rap1gds1	Rap1 GTPase-GDP dissociation stimulator 1	E9Q912
Rac3	Ras-related C3 botulinum toxin substrate 3	P60764
Hspa5	Endoplasmic reticulum chaperone BiP	P20029
Atp2b1	Plasma membrane calcium-transporting ATPase 1	G5E829
Hk1	Hexokinase-1	P17710
Elavl1	ELAV-like protein 1	P70372
Aldoc	Fructose-bisphosphate aldolase C	P05063
Sdha	Succinate dehydrogenase [ubiquinone] flavoprotein subunit, mitochondrial	Q8K2B3
Vcp	Transitional endoplasmic reticulum ATPase	Q01853
Gria2	Glutamate receptor 2	P23819
Glul	Glutamine synthetase	P15105
Atp6v1h	V-type proton ATPase subunit H	Q8BVE3

Gene Symbol	Description	Accession
Myo5a	Unconventional myosin-Va	Q99104
Oxct1	Succinyl-CoA:3-ketoacid coenzyme A transferase 1, mitochondrial	Q9D0K2
Pdha1	Pyruvate dehydrogenase E1 component subunit alpha, somatic form, mitochondrial	P35486
C3	Complement C3	P01027
Rab10	Ras-related protein Rab-10	P61027
Pebp1	Phosphatidylethanolamine-binding protein 1	P70296
Psmb6	Proteasome subunit beta type-6	Q60692
Pcmt1	Protein-L-isoaspartate(D-aspartate) O-methyltransferase	P23506
Syngr1	Synaptogyrin-1	O55100
Psma5	Proteasome subunit alpha type-5	Q9Z2U1
Slc12a5	Solute carrier family 12 member 5	Q91V14
Dbt	Lipoamide acyltransferase component of branched-chain alpha-keto acid dehydrogenase	P53395
Mdh1	Malate dehydrogenase, cytoplasmic	P14152
C4b	Complement C4-B	P01029
Syngr3	Synaptogyrin-3	Q8R191
Stxbp1	Syntaxin-binding protein 1	O08599
Cct2	T-complex protein 1 subunit beta	P80314
Vdac1	Voltage-dependent anion-selective channel protein 1	Q60932
Atp2b2	Plasma membrane calcium-transporting ATPase 2	Q9R0K7
Chchd3	MICOS complex subunit Mic19	Q9CRB9
Mri1	Methylthioribose-1-phosphate isomerase	Q9CQT1
Prdx2	Peroxiredoxin-2	Q61171
Hadha	Trifunctional enzyme subunit alpha, mitochondrial	Q8BMS1
Hspa9	Stress-70 protein, mitochondrial	P38647
Crym	Ketimine reductase mu-crystallin	O54983
Crmp1	Dihydropyrimidinase-related protein 1	P97427
Pdhb	Pyruvate dehydrogenase E1 component subunit beta, mitochondrial	Q9D051
Tkt	Transketolase	P40142
Dlg4	Disks large homolog 4	Q62108
Myl12b	Myosin regulatory light chain 12B	Q3THE2
Got2	Aspartate aminotransferase, mitochondrial	P05202
Anxa1	Annexin A1	P10107
Rab7a	Ras-related protein Rab-7a	P51150
Stub1	E3 ubiquitin-protein ligase CHIP	Q9WUD1
Gnb1	Guanine nucleotide-binding protein G(I)/G(S)/G(T) subunit beta-1	P62874
Tmem109	Transmembrane protein 109	Q3UBX0
Hspd1	60 kDa heat shock protein, mitochondrial	P63038
Hsp90b1	Endoplasmin	P08113
Kif5b	Kinesin-1 heavy chain	Q61768
Septin8	Septin-8	Q8CHH9
Eef2	Elongation factor 2	P58252
Ddah1	N(G),N(G)-dimethylarginine dimethylaminohydrolase 1	Q9CWS0
Anxa7	Annexin A7	Q07076
Rab5a	Ras-related protein Rab-5A	Q9CQD1
Septin11	Septin-11	Q8C1B7
Ap2m1	AP-2 complex subunit mu	P84091
Sdhb	Succinate dehydrogenase [ubiquinone] iron-sulfur subunit, mitochondrial	Q9CQA3
Pacsin1	Protein kinase C and casein kinase substrate in neurons protein 1	Q61644

Supplementary Table 1. List of proteins identified in Mass spectrometry interaction screen.

List of proteins identified in the proteomics dataset corresponding to Supplementary Figue 6b. Gene symbol, description, and accession numbers are provided. Note the presence of all known molecular interactors of LRRTM2 (Neurexins1-3 and Dlg4) along with GluA2 subunit of AMPARs.